Novel Optimised Structural Aluminium Cross-Sections Towards 3D Printing

Konstantinos Daniel Tsavdaridis[1], Jack Antony Hughes[2], Lukas Grekavicius[3], and Evangelos Efthymiou[4]*

[1] *Associate Professor, Institute for Resilient Infrastructure, School of Civil Engineering, University of Leeds, Woodhouse Lane, LS2 9JT, Leeds, UK (k.tsavdaridis@leeds.ac.uk)*

[2] *Graduate Engineer, Robert Bird Group, Level 2 Harling House, 47-51 Great Suffolk St, London SE1 0BS (jack.hughes@robertbird.com)*

[3] *Graduate Engineer, Cundall, 4th Floor, Partnership House, Regent Farm Road, Gosforth, Newcastle upon Tyne, NE3 3AF (l.grekavicius@cundall.com)*

[4] *Assistant Professor, Institute of Metal Structures, Department of Civil Engineering, Aristotle University of Thessaloniki, GR 54124, Thessaloniki, Greece (vefth@civil.auth.gr)*

[*]*Corresponding and Presenting Author*

Keywords: Manufacturing processes, aluminium structural members, novel cross-section design, structural topology optimisation, SIMP technique, extrusion, 3D Printing.

Abstract

In the last decades, the deployment of aluminium and its alloys in engineering fields has been increased significantly, due to the material's special features accompanied by supportive technological and industrial development such as the extrusion manufacturing method. However, the extent of aluminium structural applications in building activities is still rather limited, and barriers related to strength and stability issues prevent its wider use. In the context of topology optimisation, appropriate design in aluminium cross-sections can overcome inherent deficiencies, such as the material's low elastic modulus.

The current study investigates the application of structural topology optimisation to the design of aluminium beam and column cross-sections, through a combination of 2D and 3D approaches, with focus on post-processing and manufacturability. Ten unique cross-sectional profiles are proposed based on structural testing through Finite Element Analysis (FEA). Conclusions attempt to highlight the general characteristics of the optimised aluminium cross-sections as well as the benefits of the using extrusion and 3D printed manufacturing methods in order to realise these results.

Introduction

Aluminium is a unique material that has the potential of competing within the construction industry. Successful application of aluminium alloys in structural engineering is connected to its inherent physical and mechanical properties: low density, which allows reduced loads on foundations and easier construction process; excellent corrosion resistance, which reduces its maintenance requirements; and the extrusion process, which allows the production of members with efficient and optimised cross-sections [1]. In particular, although available for some other non-ferrous metals, such as brass and bronze, it is with aluminium that the extrusion process has become a major manufacturing method [2]. The extrusion process allows aluminium sections to be formed in an almost unlimited range of shapes, while a significant advantage is the ability to produce sections that are very thin relative to their overall size [3]. Additive manufacturing and in particular 3D printing process delivers similar advantages in the design and fabrication of monolithic structural elements of complex shapes, and in particular those are irregular along the length of the member.

Aluminium cross-sections are separated into four classes based on b/t ratio limits of reinforced and un-reinforced parts. When compared to standardised steel sections, aluminium cross-sections are often asymmetric, more complex, contain thin walls and are reinforced with ribs, bulbs and lips [4]. Local instability is, therefore, the governing factor when designing such sections. Another factor that is linearly related to buckling resistance of beams and columns is the stiffness of cross-sections (*EI*).

To compensate for the low elastic modulus and achieve higher stiffness, the moment of inertia has to be increased. When considering standard shapes this would result in deeper and slenderer sections, which are more susceptible to buckling. However, sections obtained through advanced topology optimisation techniques can achieve a high I-value with an optimal amount of material.

Structural topology optimisation is based on the principle of optimising the number and size of openings within a design space, in order to satisfy the applied loading and constraints. There are numerous topology optimisation techniques available in the literature. The currently most popular one is the Solid Isotropic Material Penalisation (SIMP) technique, which is based on discretising the design domain into finite elements and utilising FE analysis to vary the densities in each element. Depending on the intensity of stresses, the elements are characterised as being low, high or intermediate density [5]. The process is iterative until convergence is reached.

Topologies may resemble complex natural forms; therefore, it is often up to the designer to interpret them. Interpretation is a crucial part of the overall optimisation process and needs to be performed carefully with consideration of manufacturing and practicality factors. This has been unaddressed in the existing literature [6, 7, 8], which is limited to a selection of a few load conditions and there have not been any attempts made yet at optimising aluminium cross-sections. Therefore, this study aims to utilise the complimentary of the co-authors in optimisation and aluminium and propose new efficient structural shapes by conducting cross-sectional topology optimisation analysis of 6063-T6 aluminium alloy beams and columns. It is intended to achieve a minimum possible weight with maximum stiffness, as weight savings can render significant reductions in manufacturing and construction costs, as well as environmental impact.

Manufacturing processes

Aluminium is presently extracted exclusively from bauxite, however, it also exists in other minerals within the earth's crust to make it the third most abundant element. Combined with the high recyclability rate of the end product, this ensures that there is adequate material for continued sustainable construction for an almost indefinite period.

Once combined with its alloying elements, the new material is classed as being a casting or wrought alloy, dependent on whether it is to be melted before casting. As a result, most hot rolled and extruded applications utilise wrought alloys. The heat treatment process is then followed by quenching and ageing, during which the majority of hardening occurs.

The current state-of-the-art manufacturing process for aluminium member is the extrusion process Fig. 1(a)-left. The extrusion process creates cross-sectional shapes by forcing hot metal, in the form of a billet, through an opening called a die (e.g., porthole and bridge dies). The corresponding cross-section then matches the profile of the die, regardless of it complexity. This enables designers to create specific sections to meet requirements, simply by producing the appropriate die; such as the complex shapes shown in Fig. 1(a)-right. This method provides a relatively high quality result with national specifications allowing a deviation of approximately 5% from the nominal thickness.

The cost influencing criterial as being very similar to those for rolled sections, however, specific costs may vary dramatically for bespoke die designs. In general, costs for hollow sections have been reported as being up to five times more expensive than solid or open profiles. Cheaper manufacture methods are available, such as shell casting rather than die casting, however, larger tolerances for imperfection may be expected.

On the other hand, recently, designers are pushing technologies to realise the full potential of 3D printing and overcome material quality, monitoring, and size limitations (Fig. 1(b) – the biggest 3D printing for metallic members). This method of fabrication is a new process of making a 3D solid object directly from a digital model. It is an additive process where successive layers of material are laid down in a controlled way to achieve the desired (optimised) shape, replacing traditional machining techniques, dealing with material removal through cutting and splitting, sawing/drilling/rounding off, and CNC turning/milling. There are three 3D printing techniques such as: (i) Extrusion type – Fuse Deposition Modelling (FDM) used for thermoplastics: PLA, ABS, nylon,

alumide (a mix of nylon and aluminium); (ii) Granular type – Selective Laser Sintering (SLS) used for thermoplastics, metal powders, and ceramic powders; (iii) Liquid type – Multi Jet Modelling (MJM) used for acrylic plastic.

The cost of the 3D printing is comparable to the one of the extrusion process, but cannot be precisely evaluated since massive production is required while the industry is still experimenting. For this reason, this paper contributes to the effort demonstrating the need for larger scale 3D printers as well as focus on high production of structural elements through comprehensive comparisons between typical structural aluminium cross-section members that can be produced by extrusion process, and fully optimised structural aluminium members that can only be manufactured by 3D printers. Table 1 below, is the first attempt to compare the pros and cons of the two aforementioned manufacturing processes and draw the overall picture of the current state-of-the-art.

Figure 1(a). Extrusion process (left) and products (right)

Figure 1(b). Biggest 3D printer (left) and manageable complexity of product design (right)

Table 1. Overview of manufacturing processes

	Extrusion	3D Printing
Advantages	• Length (long span, <30m) • Quick production (20-70m/min) • Similar cost to cold forming • No trimming or milling is required • Very few imperfections and residual stresses	• No supply chain is required • Achieve any optimised complex shape (decrease weight to stiffness ratio)

Disadvantages	• Constant cross-section along the length of the member • Need pre-production of the die • Can be five times more expensive than solid or open profile	• Size limitations (so far) • Brittle performance in certain occasions • Cracking control is required • Roughness control is required (direction dependent) • Time expensive process • Certain models only suitable for limited temperature range

Topology Optimisation Approach

This research undertook a combination of approaches, in order to consider all necessary degrees of freedom identified in Fig. 2. A 2D approach was used to identify a wide variety of cross-sectional profiles, however this approach did not consider variations in bending and shear along the length of the member. A 3D approach was then used to provide a series of comparative cross-sectional slices, to capture the effect of this variation. All optimisation was performed using Altair Engineering's software package HyperWorks v13.0. Through this, more than 40 different combinations of loading and support conditions were analysed. Loading conditions were chosen with reference to the standard cross-section classification procedure for outstand and internal compression elements given by codified provisions [9].
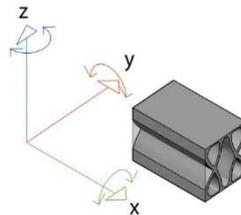

Figure 2. Considered directions of rotation and translation

Linear static analysis was performed on an elastic material model with the following properties: Young's modulus of 70 GPa, Poisson's ratio of 0.3, shear modulus of 27 GPa and density of 2700 kg/m^3. Shell elements with a nominal size of 1 mm and solid elements with a nominal size of 5 mm were used to model the 2D and 3D members, respectively. All models have been optimised for minimum compliance (therefore maximum stiffness) subject to a constraint on the final volume fraction of 0.275. Manufacturability is addressed through constraints on symmetry and a minimum member size of 7 mm. This optimisation problem has been validated in both the 2D and 3D cases. When compared to the results obtained in existing literature [6, 8] a close agreement of the patterns has been identified.

Identical analysis has been performed to compare topologies obtained with aluminium and steel. Aluminium alloy 6063-T6 (with a tensile strength of 245 N/mm^2) was compared to grade S355 steel with Young's modulus of 210 GPa and Poisson's ratio of 0.3. Identical topologies reveal that the optimisation constraints and geometry are dominant, therefore the results are applicable to both materials.

A 100x100mm square section has been chosen as the initial design domain in order to provide maximum flexibility in the resulting topologies. So as to provide a comparison however, sections with aspect ratios of 100x200mm and 200x100mm have also been optimised. Fig. 3 demonstrates

that very similar density plots are achieved regardless of the aspect ratio, therefore the sections may be adapted into similar forms as required.
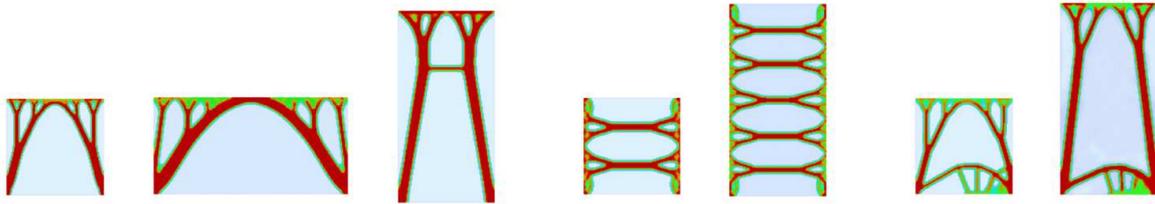

Figure 3. Topologies of cross-sections with various aspect ratios

Topology optimisation results must be carefully interpreted into a suitable structure. The results are highly sensitive to geometry, so a method of post-processing multiple results to allow for these sensitivities is proposed. The contour plots shown previously have been smoothed with a density threshold of 0.3 using Altair Engineering's OSSmooth and extracted into AutoCAD. Afterwards, the results from multiple loading and support conditions have been overlaid and presented in a form appearing similar to x-rays. These show the most frequently stressed material to be darker in colour and allow for the interaction of various load cases to be considered.

Optimisation processes for lightweight structures typically result in thin-walled cross-sections. When combined with aluminium's lower modulus of elasticity, local instability modes including distortional and local buckling are typically dominant. In order to minimise the likelihood of these failures, optimal placement of compression members and stiffeners is of vital importance. Using the described post-processing method, this stability criterion should be satisfied by comparing the typical stresses in cross-sections subjected to torsion, compression, yielding and one or two plane buckling.

Topology Optimisation of Cross-sections

Beams. Pinned supports to 2 and 4 nodes are compared, in order to propose sections suitable for simply supported and fixed beams respectively. Major axis bending and torsion have then been applied. Fig. 4 shows 5 beam cross-sections developed after processing. Section properties are then presented in Table 2. For beams that are primarily subjected to bending about one axis only, the proposed sections are symmetric about one plane. Asymmetric cross-sections are also included for additional stiffness when subjected to torsion. Regardless of the applied symmetry, it is noticed that the topology results have a similar moment of inertia about both axes.
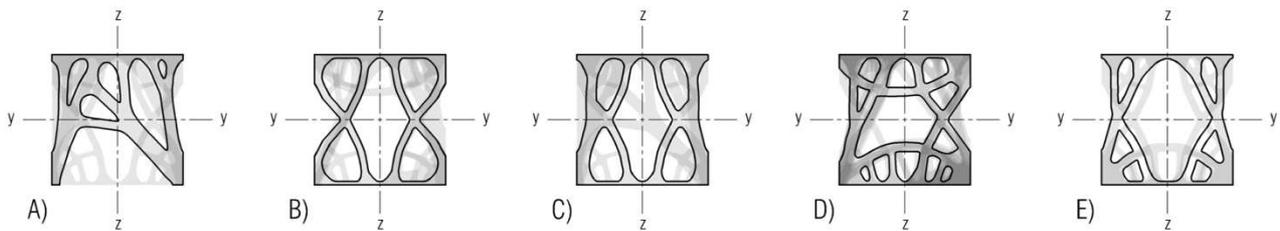

Figure 4. Post-processing of beam cross-sections

Table 2. Beam section properties

Section	A	B	C	D	E
Area [cm^2]	44.39	30.32	39.43	48.84	37.82
Moment of inertia, y [cm^4]	340.26	337.32	399.50	528.69	436.66
Moment of inertia, z [cm^4]	448.14	312.46	423.15	479.10	426.65

3D optimisation was performed on a 2 m extruded 100mm square beam, with total of six different loading and support combinations; including the case of fixed supports and a uniformly distributed load to the top flange as shown in Fig. 5(a). These reveal constant cross-sections such as elliptical hollow profile across 45-50% of the length of the beam. The remaining portion shows three distinct

regions of low stress at approximately ¼, ½, and ¾ of the span, as seen in Fig. 5(b). These regions are observed to correspond with the intersections of the lines of principal tensile and compressive stresses in a homogeneous beam.
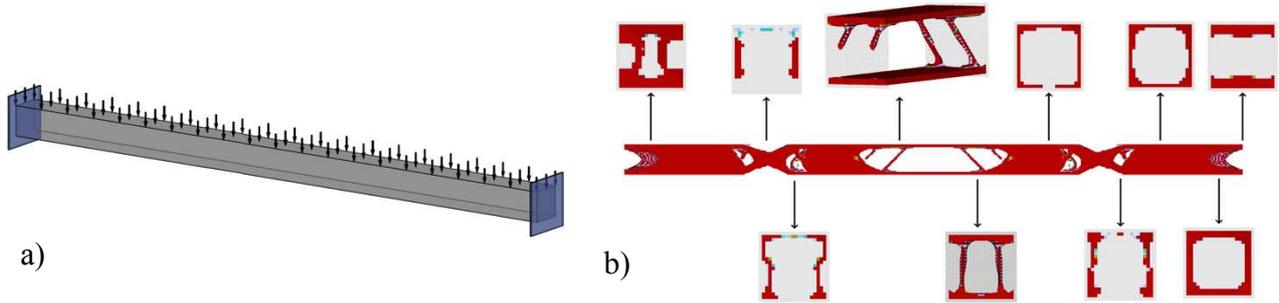

Figure 5. 3D optimisation input (a) and resulting topology with cross-sectional slices (b)

Columns. Optimisation of 2D column cross-sections with various support and loading conditions was initially attempted. Sections with two and four corner pin supports were analysed, subjected to axial compression, which include failure by yielding and one or two plane buckling. Column cross-sections found in practice are most commonly symmetric and have high buckling resistance about one or more axes depending on specific applications, hence this logic is followed in developing the final cross-sections shown in Fig. 6. The first attempt considers a column under pure compression, such cross-sectional profile would reach its yield stress limit and experience material failure. The shape resembles a standard double webbed compound column cross-section used in the industry. The second attempt considers column failure due to buckling. Fig. 6 B and C represent a cross-sectional profile of a column having high stiffness in the y-y axis. The cross-sections are a combination of resulting stress plots with loading replicating compression and bending of a member as it buckles. Therefore, they are applicable in cases when an eccentric axial load or a moment are applied triggering one plane buckling. Sections presented in Fig. 6 D and E are resistant to compression and buckling in two axes. These profiles have equal stiffness in both axes and appear more resistant to local buckling. The section properties are presented in Table 3.
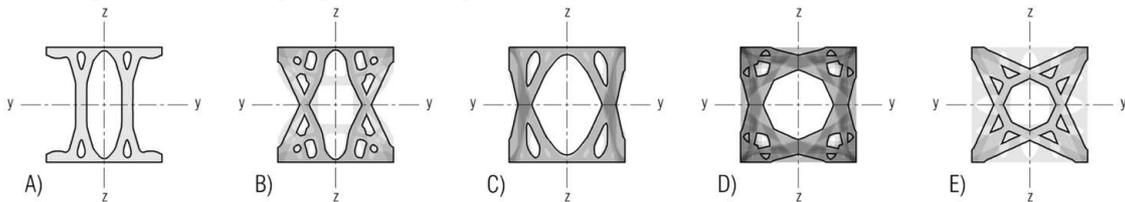

Figure 6. Post-processing of column cross-sections

Table 3. Column section properties

Section	A	B	C	D	E
Area [cm^2]	35.36	49.95	52.00	59.13	49.10
Moment of inertia, y [cm^4]	461.63	565.23	582.67	608.38	442.67
Moment of inertia, z [cm^4]	224.58	449.33	578.80	608.38	442.67

3D optimisation was performed on a 2 m extruded 100x100 mm square column with fixed-pinned supports as shown in Fig. 7(a). An axial compressive load was applied at the top and loads triggering buckling in two planes – in the middle of the member. Symmetry manufacturing constraint was applied to the model about y-y and z-z axes. When subjected to two plane buckling the column developed concentrations of material at the four corners (Fig. 7), resembling a box section at multiple locations along the length of the member. Formation of a web connecting the flanges is also observed in the middle of the member at the location of the lateral load. The box shape of the cross-section could be related to the fully symmetric profiles obtained through 2D optimisation (Fig. 6 D and E).
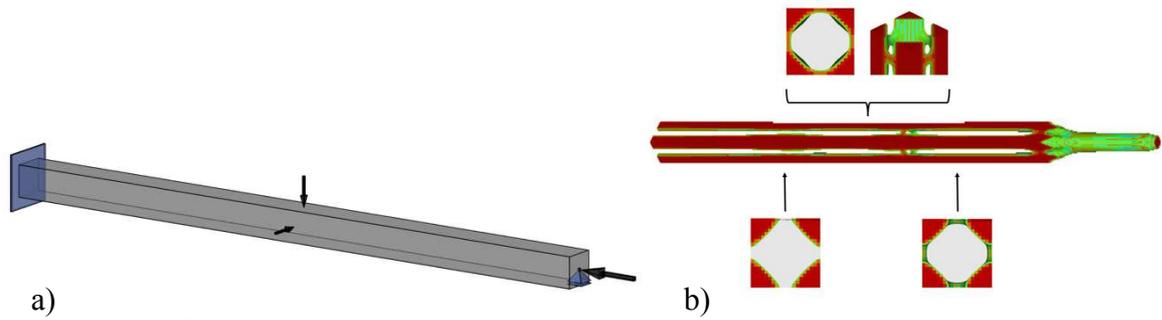
Figure 7. 3D optimisation input (a) and resulting topology with cross-sectional slices (b)

Finite Element Analysis

Analysis Parameters. Finite element analysis (FEA) software ANSYS v14.0 is adopted in this study to assess the performance of the unique cross-sectional shapes. Geometrical and material non-linear analysis was employed, which takes into account the plastic behaviour of aluminium.

Results - Beams. Two of the optimised beam cross-sections developed have been tested through the FE analysis. In order to provide a reliable benchmark for how suitable the optimisation method is for developing new cross-sections, the two chosen have been compared against a selection of three conventional and two additional novel cross-sections, each of which are shown in Fig. 8. SHS and UB profiles have been included within the compared cross-sections as they are also available as steel profiles. A conventional Y-profile has then also been included, as an additional section that is only used in aluminium. Two novel cross-sections are then additionally included within the comparison, one of which is the result of previous optimisation studies by Kim and Kim [10]. As in the optimisation analysis, the models adopt a 100mm square cross-section, and have been tested with lengths of both 2m and 1m in order to consider both extremities of span to depth ratios with 20 and 10.
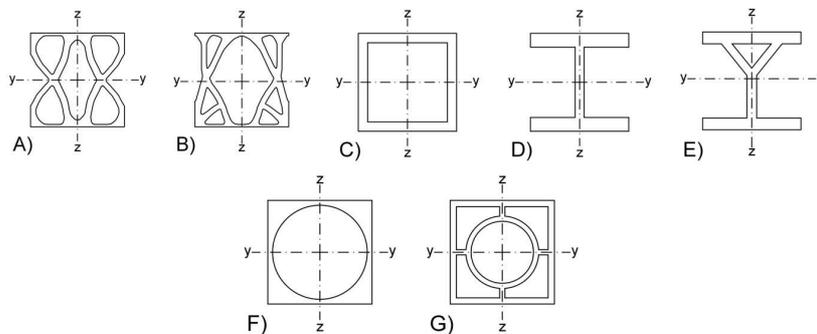

Figure 8. Beam Cross-Sections Employed in Finite Element Analysis

All beams analysed have been subject to a uniformly distributed pressure to the top flange, along with a variety of two different support conditions. The first set of models have been analysed with fully fixed ends to prevent both translation and rotation, whilst the second set was modelled using a pinned bottom flange.

The members with 2m length experienced significant plastic deformation and clearly demonstrate that serviceability criteria are the critical design aspect. Each of the members was able to resist the maximum applied load of 2MPa, however they show significant mid-span deflections that are unacceptable in practice. At this ultimate load, the optimised cross-section A shows the least deflection, and the conventional SHS showing the most. Due to the large deflections however, the failure load of the members has been taken as that at a serviceability limit of the deflections of span/250. At the 8mm deflection limit imposed by this criterion the performance of the various cross-sections dramatically differs, with the conventional sections marginally out-performing the optimised profiles. Due to the large mid-span deflections seen in the beams analysed with span-depth ratios of 20, it was considered necessary to analyse a series of stockier beams at span-depth ratios of 10. Pinned

supports have been used in this set of results, to enable failure of the cross-sections at the high stress concentrations observed near the supports. These members were subjected to identical loading, and due to their alternate dimensions experienced much more acceptable levels of deflection at the ultimate load. The failure loads and corresponding deflections are presented in Table 4, along with the load-deflection curves in Fig. 9. The results show a much larger variation in the experienced deflections and failure loads, and therefore enable a clearer comparison when looking at the load-deflection curve.

Table 4. Analysis Results for 1m Pinned Beams

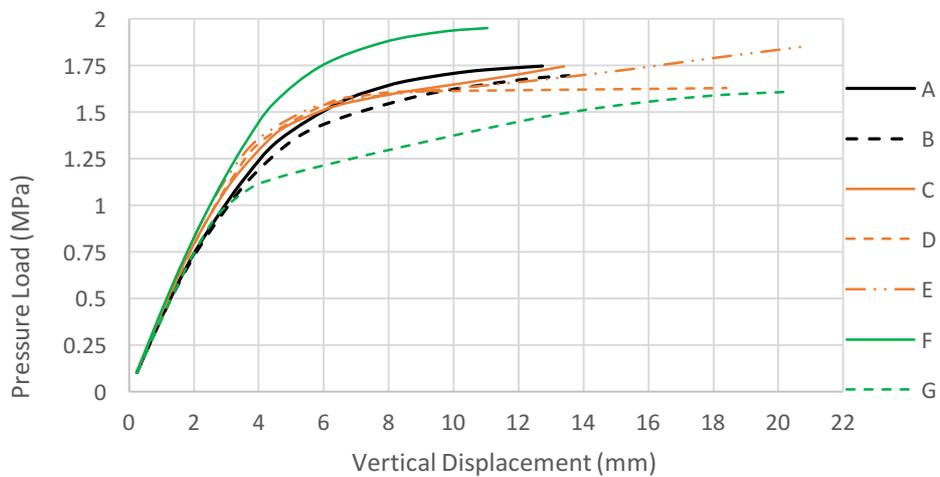| Section	A	B	C	D	E	F	G
Ultimate Pressure [N/mm^2]	1.75	1.69	1.82	1.63	1.89	1.95	1.61
Von-Mises Stress [MPa]	179.91	169.81	169.91	179.67	177.16	169.80	185.52
Mid-span deflection [mm]	12.98	13.69	16.82	18.49	23.93	11.45	20.83

Figure 9. Load-Deflection Curves for 1m Pinned Beams

Both optimised cross-sections A and B have performed well in this comparison, and show relatively low levels of deflections. Novel cross-section F is quite significantly the most efficient however, showing both the highest failure load and the lowest deflection simultaneously.

Results - Columns. Two of the optimised shapes were chosen to be analysed; one with large stiffness in one axis and one with equal stiffness about both axes. In addition, two conventional and two novel shape sections with similar mass were chosen for a comparative analysis similarly to the beams. The tested cross-sectional profiles are shown in Fig. 10.
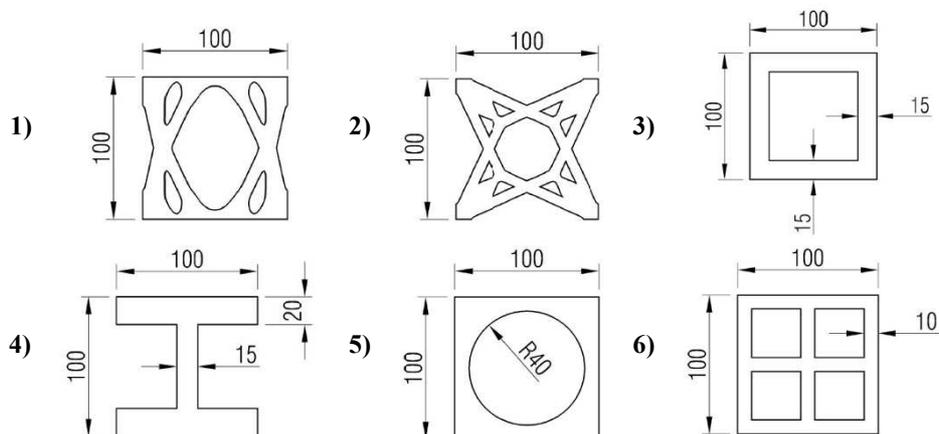

Figure 10. Column Cross-Sections Employed in Finite Element Analysis

The models were constrained with pined support conditions. All translational degrees of freedom were restrained at both ends, apart from the one in the axial direction at one end. A compressive axial load was applied to the column extrusions by specifying pressure on the top face. The critical buckling loads and their corresponding deflections were extracted for all cross-section models (shown in Table 5). The performance of all sections is also presented in the load-deflection curve Fig. 11.

Table 5. Analysis Results for 2m Pinned Columns

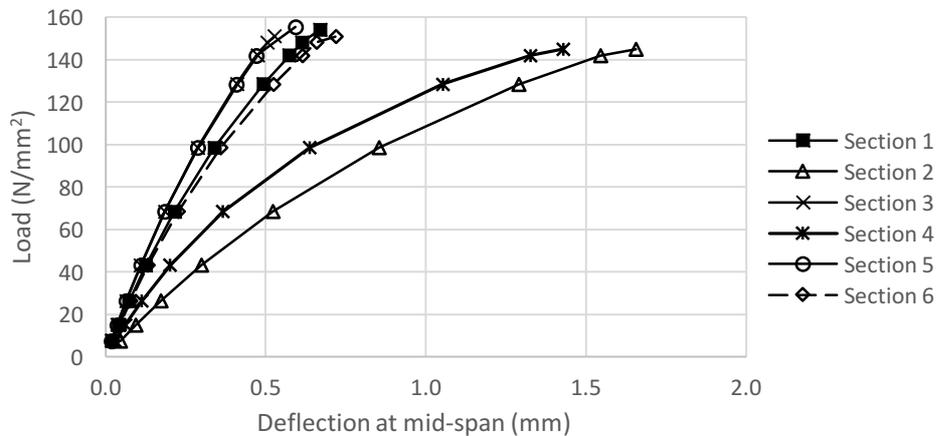| Section	1	2	3	4	5	6
Ultimate load [N/mm^2]	154.09	144.94	151.01	144.94	155.44	151.01
Deflection at mid-span [mm]	0.67	1.66	0.53	1.43	0.59	0.72
Max lateral deflection [mm]	0.72	1.80	0.58	1.58	0.64	0.78
Vertical deflection [mm]	4.43	4.29	4.38	4.27	4.47	4.40

Figure 11. Load-Deflection Curves for 2m Pinned Columns

A clear separation between Sections 2 and 4, and the rest of the specimens is observed with Sections 2 and 4 indicating the worst performance. Despite the same load limit, Section 2 shows a worse response due to the largest magnitude of the lateral deflection at mid-span. Even though Section 4 (H-section) column stiffness in the minor axis (z-z) is lower than any other sections, it does not experience the largest deflection. Instead, Section 2 was the one that performed poorly in terms of lateral deflection. Thus, it can be concluded that Section 2 has the smallest stiffness and load-capacity out of all the specimens, despite being one of the two optimised cross-sectional profiles. Analysis results for Section 5 indicate the best performance. This box section with a circular hollow, despite possessing a smaller cross-sectional area, performed better than a standard box section (Section 3). Section 1 – one of the two optimised cross-sections – indicated a better performance than most within the comparison. Therefore, Section 1 is only slightly weaker than the stiffest (Section 5). Sections 3 and 6 also performed relatively well. Surprisingly, a square box section without internal stiffeners (Section 3) performed better than a square box section with stiffeners (Section 6).

Concluding Remarks

Extrusion processes and 3D printing provides engineers the freedom to design structural products that cannot be manufactured with traditional ways such as the typical steel members made through a cold or a hot formed process. Especially, the most recently developed 3D printed manufacturing process, is a process of adding material, as opposed to subtracting material in the classic methods, and allows for more intricate optimised shapes that inherently provide strength and stiffness. This has given engineers an unprecedented chance to design lighter, more organic looking products which are aesthetically pleasing and practical and fully exploit the advanced optimisation tools to design new structural elements. Moreover, 3D printing offers another benefit to design engineers; no supply chain

is required. The final product does not need welding and bolting anymore and this guarantees its long lasting performance.

In this paper, new cross-sectional topologies for aluminium structural members have been investigated through structural topology optimisation. A series of unique cross-sections have been generated using the SIMP technique, subject to different loading and support conditions. A tailored method for post-processing the 2D planar results is presented which aimed to address stability and manufacturability criteria. In this way, different density plots have been overlaid to identify the most frequently stressed areas of the cross-section, which resulted in five novel section profiles for beams and columns. A 3D optimisation approach was also presented to identify correlation between 2D and 3D results.

Both approaches for beams and columns predominantly result in complex hollow-like sections, with a large central opening and other smaller peripheral openings. Due to the square (but also the rectangular) design domain, most sections have a similar moment of inertia about both axes. Beam sections have an approximately central neutral axis despite only one plane of symmetry has been applied. As it was expected, all column sections are symmetric about both axes and have high or equal stiffness about one or two axes, respectively. Four of the optimised cross-sections are compared with a range of more conventional aluminium profiles under static loads using a FEA package. Results for beams and columns are presented, and indicate that the optimised cross-sections are able to provide a large stiffness and out-perform some conventional profiles, with one typology demonstrating the best efficiency for both beams and columns. The next step of this research project is to experimentally test the optimised scaled beam and column members manufactured through extrusion and 3D printing processes, with scope to investigate their structural performance under bending, compression (and combined actions) as well as fatigue. Due to the 3D printing process, surface roughness and crack control should be also checked at that stage in order to achieve similar stiffness in static and cyclic loads. Thus, safety factors will be employed in an attempt to allow Eurocode 9 for the design of such 3D printed and optimised aluminium structural elements.

References

[1] F.M. Mazzolani, Aluminium alloy structures, CRC Press, London, 1994.

[2] U. Muller, Introduction to structural aluminium design, Whittles Publishing, Scotland, UK, 2011.

[3] J. Dwight, Aluminium design and construction, E & FN SPON, London, UK, 1999.

[4] F. M. Mazzolani (ed), Aluminium structural design, CISM- International center for mechanical sciences-Courses and lectures No 443, Springer-Verlag WienNewYork, Udine, Italy, 2003.

[5] M.P. Bendsoe, O. Sigmund, Topology optimization: theory, methods, and applications, Springer Science & Business Media, Berlin, 2013.

[6] K. Anand, A. Misra, Topology Optimization and Structural Analysis of Simple Column and Short Pressurized Beams Using Optimality Criterion Approach in ANSYS, IRJET 02(3) (2015) 1408-1415.

[7] B. Bochenek, K. Tajs-Zielińska, Minimal compliance topologies for maximal buckling load of columns, Struct Multidisc Optim, 51(5) (2015) 1149-1157.

[8] R.H. Zuberi, Z. Zhengxing, L. Kai, Topological optimization of beam cross section by employing extrusion constraint, Proceedings of ISCM II and EPMESC XII 1233(1) (2010) 964-969.

[9] CEN/TC250/SC9, EN 1999-Eurocode 9: Design of aluminium structures- Part 1-1: General structural rules, CEN-European Committee for Standardisation, Brussels, Belgium, 2007.

[10] Kim, Y. and Kim, T. (2000). Topology optimization of beam cross sections. International Journal of Solids and Structures, 37(3), pp.477-493.